

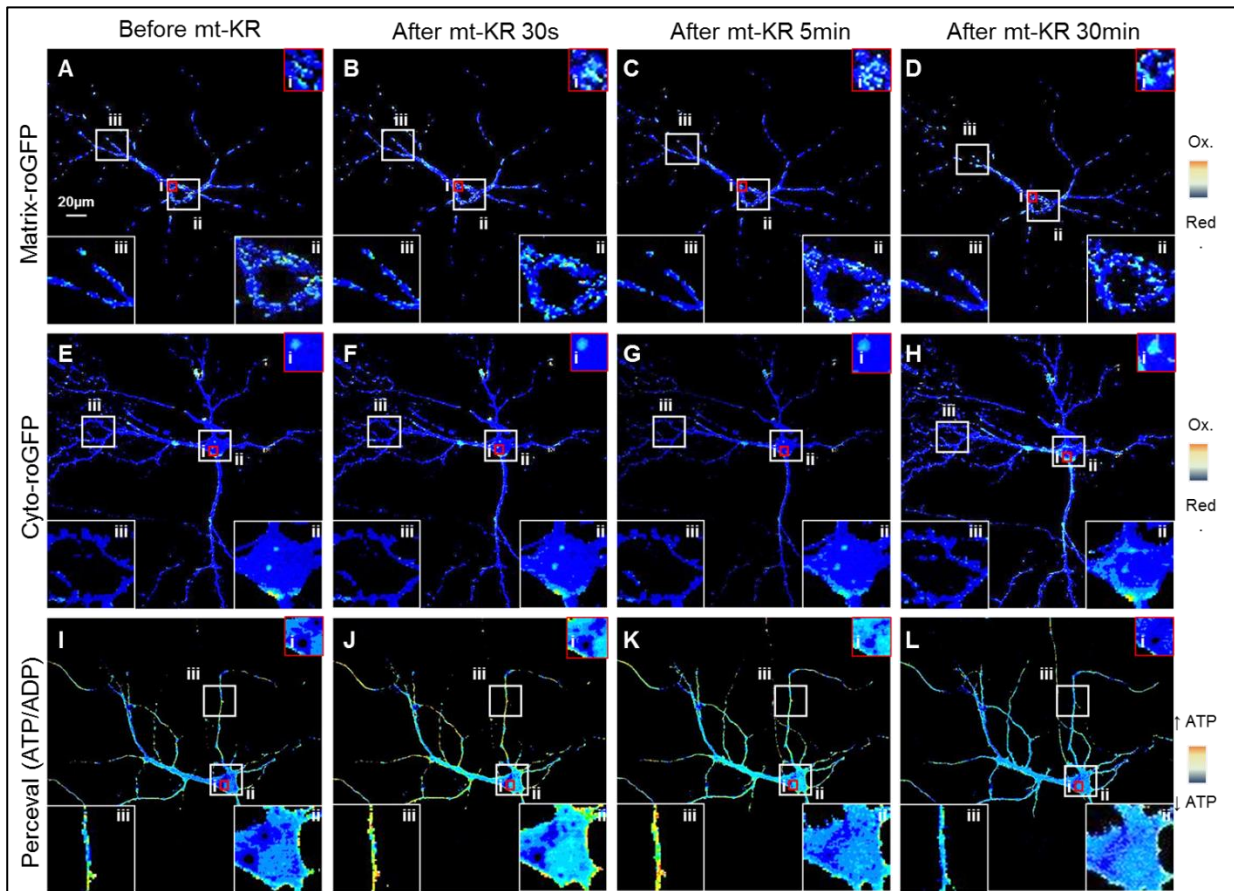
ISCI, Volume 6

Supplemental Information

**Local Oxidative Damage in the Soma
and Dendrites Quarantines Neuronal
Mitochondria at the Site of Insult**

Amandine Grimm, Nadia Cummins, and Jürgen Götz

Supplementary figures and legends



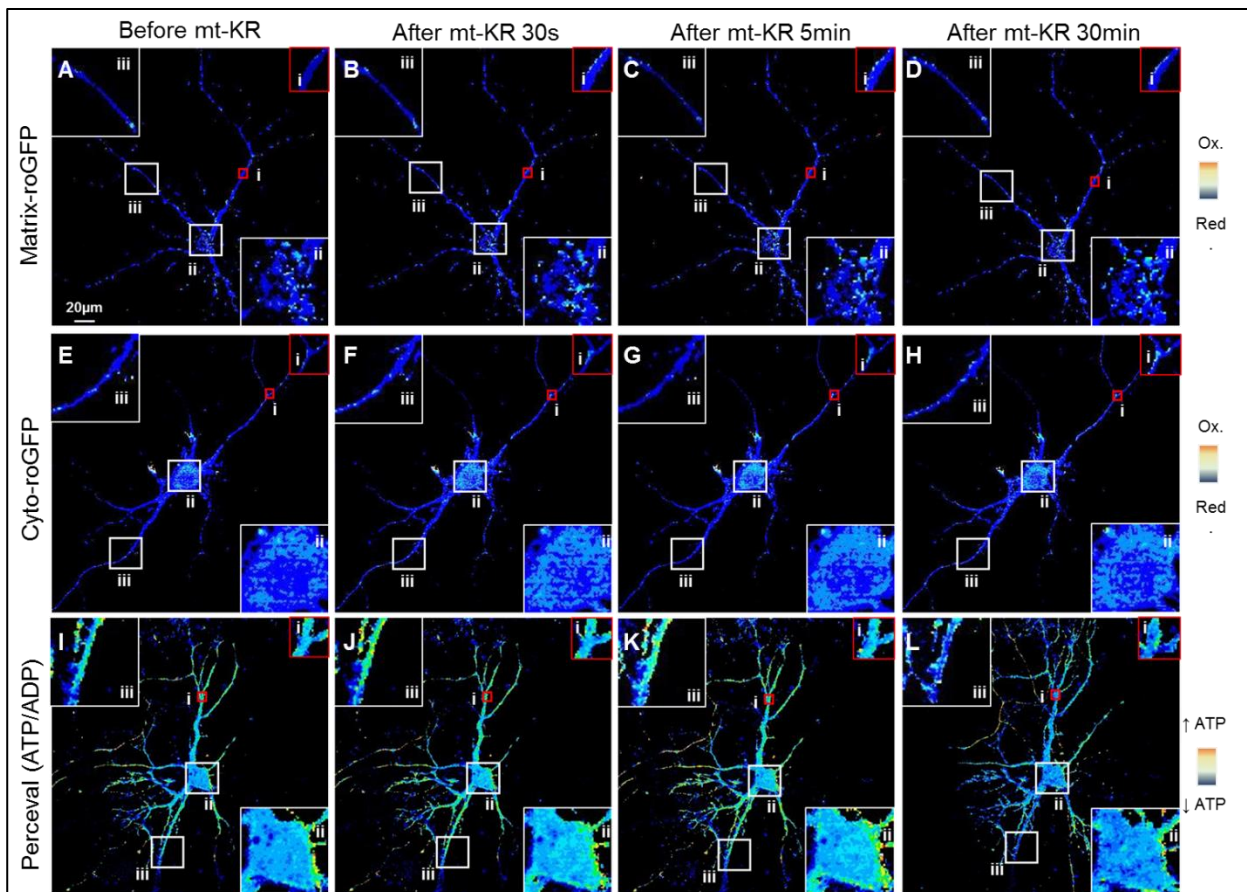
Supplementary Figure 1, related to Figure 3 B-D. Somatodendritic redox state and ATP/ADP ratio after focal mt-KR activation in the soma

A-D. Fluorescence ratio (405 nm/488 nm) of the matrix-roGFP protein before (A), 30 s after (B), 5 min after (C), and 30 min after (D) mt-KR activation in the soma.

E-H. Fluorescence ratio (405 nm/488 nm) of the cytosolic roGFP protein before (E), 30 s after (F), 5 min after (G), and 30 min after (H) mt-KR activation in the soma.

I-L. Fluorescence ratio (488 nm/405 nm) of the Perceval protein (ATP/ADP ratio) before (I), 30 s after (J), 5 min after (K), and 30 min after (L) mt-KR activation in the soma.

For each representative image, a zoomed-in image (400%) is shown for the simulated zone (i), the soma (ii) and a dendrite (iii). mt-KR: mito-KillerRed



Supplementary Figure 2, related to Figure 3 F-H. Somatodendritic redox state and ATP/ADP ratio after focal mt-KR activation in the dendrite

A-D. Fluorescence ratio (405 nm/488 nm) of the matrix-roGFP protein before (A), 30 s after (B), 5 min after (C), and 30 min after (D) mt-KR activation in the dendrite.

E-H. Fluorescence ratio (405 nm/488 nm) of the cytosolic roGFP protein before (E), 30 s after (F), 5 min after (G), and 30 min after (H) mt-KR activation in the dendrite.

I-L. Fluorescence ratio (488 nm/405 nm) of the Perceval protein (ATP/ADP ratio) before (I), 30 s after (J), 5 min after (K), and 30 min after (L) mt-KR activation in the dendrite.

For each representative image, a zoomed-in image (400%) is shown for the simulated zone (i), the soma (ii) and a non-stimulated dendrite (iii). mt-KR: mito-KillerRed

Supplementary Table 1, related to Figure 3. Statistical analysis of somatodendritic redox state and ATP/ADP ratio changes after focal mt-KR activation in the soma and dendrites.

		Time (min)												
		0.5	1	1.5	2	2.5	3	3.5	4	4.5	5	30	30.5	
Soma	Mitoch. redox state	ROI in soma	**	****	**	**	*	*	*	*	*	ns	***	***
		Around ROI	ns	ns	ns	ns	ns	ns	ns	ns	ns	ns	ns	ns
		Soma	ns	ns	ns	ns	ns	ns	ns	ns	ns	ns	ns	ns
		Prox. Dend.	ns	ns	ns	ns	ns	ns	ns	ns	ns	ns	ns	ns
		Dist. Dend.	ns	ns	ns	ns	ns	ns	ns	*	*	*	ns	ns
		Total	ns	ns	ns	ns	ns	ns	ns	ns	ns	ns	ns	ns
	Cytosolic redox state	ROI in soma	ns	ns	ns	ns	ns	ns	ns	ns	ns	ns	***	***
		Around ROI	ns	ns	ns	ns	ns	ns	ns	ns	ns	ns	*	*
		Soma	ns	ns	ns	ns	ns	ns	ns	ns	ns	ns	*	*
		Prox. Dend.	ns	ns	ns	ns	ns	ns	ns	ns	ns	ns	ns	ns
		Dist. Dend.	ns	ns	ns	ns	ns	ns	*	*	*	*	ns	*
		Total	ns	ns	ns	ns	ns	ns	*	*	*	**	ns	ns
	ATP/ADP	ROI in soma	ns	ns	ns	ns	ns	ns	ns	ns	ns	ns	**	**
		Around ROI	****	ns	ns	ns	ns	ns	ns	ns	ns	ns	ns	ns
		Soma	****	ns	ns	ns	ns	ns	*	*	*	*	ns	ns
		Prox. Dend.	**	ns	ns	ns	*	**	***	***	****	****	ns	ns
		Dist. Dend.	***	*	**	**	****	****	****	****	****	****	**	***
		Total	***	ns	ns	ns	**	***	****	****	****	****	ns	*
Dendrites	Mitoch. redox state	ROI in soma	**	****	***	***	**	*	ns	ns	ns	ns	ns	ns
		Around ROI 1	ns	ns	ns	ns	ns	ns	ns	ns	ns	ns	ns	ns
		Around ROI 2	ns	ns	ns	ns	ns	ns	ns	ns	ns	ns	ns	ns
		Soma	ns	ns	ns	ns	ns	ns	ns	ns	ns	ns	ns	ns
		Prox. Dend.	ns	ns	ns	ns	ns	ns	ns	ns	ns	ns	ns	ns
		Dist. Dend.	ns	ns	ns	ns	ns	ns	ns	ns	ns	ns	ns	ns
		Total	ns	ns	ns	ns	ns	ns	ns	ns	ns	ns	ns	ns
	Cytosolic redox state	ROI in soma	ns	ns	ns	ns	ns	ns	ns	ns	ns	ns	****	****
		Around ROI 1	ns	ns	ns	ns	ns	ns	ns	ns	ns	ns	*	*
		Around ROI 2	ns	ns	ns	ns	ns	ns	ns	ns	ns	ns	ns	ns
		Soma	ns	ns	ns	ns	ns	ns	ns	ns	ns	ns	ns	ns
		Prox. Dend.	ns	ns	ns	ns	ns	ns	ns	ns	ns	ns	ns	ns
		Dist. Dend.	ns	ns	ns	ns	ns	ns	ns	ns	ns	ns	ns	ns
		Total	ns	ns	ns	ns	ns	ns	ns	ns	ns	ns	ns	ns
	ATP/ADP	ROI in soma	ns	ns	ns	ns	ns	ns	ns	ns	ns	ns	ns	****
		Around ROI 1	*	ns	ns	ns	ns	ns	ns	ns	ns	ns	ns	****
		Around ROI 2	***	ns	ns	ns	ns	ns	ns	ns	ns	ns	ns	**
		Soma	***	ns	ns	ns	ns	ns	ns	ns	ns	ns	ns	****
Prox. Dend.		***	ns	ns	ns	ns	ns	ns	*	*	*	ns	ns	
Dist. Dend.		**	ns	ns	*	**	***	****	****	****	****	ns	ns	
Total		***	ns	ns	ns	*	**	**	**	**	**	ns	ns	

The table displays the statistical analysis relative to the Figure 3 (B-D, F-H). Two-way ANOVA (repeated measurements) and Dunnet's multiple comparison test versus baseline (0 min); *P<0.05; **P<0.01; ***P<0.001; ****P<0.0001.

Supplementary Table 2, related to Figure 3. Pearson correlation between the mitochondrial redox state and ATP/ADP ratio after focal mt-KR activation in the soma and dendrites

	Area	Slope	R square	P value
Soma	ROI in soma	-0.6045	0.2721	0.0675
	Around ROI	-2.194	0.6882	0.0005
	Soma	-2.045	0.7915	<0.0001
	Prox. Dend.	-2.578	0.6964	<0.0001
	Dist. Dend.	-1.83	0.8059	<0.0001
	Total	-1.55	0.7682	<0.0001
Dendrites	ROI in dendrites	1.1981	0.006577	0.7923
	Around ROI 1	0.00345	0.000071	0.9781
	Around ROI 2	-2.501	0.3791	0.0251
	Soma	-3.971	0.9467	<0.0001
	Prox. Dend.	-1.999	0.8052	<0.0001
	Dist. Dend.	-1.456	0.3223	0.043
	Total	-2.457	0.6414	0.001

The table displays the statistical analysis relating to Figure 3 (I, J).

ROI: region of interest.

TRANSPARENT METHODS

Cell culture

Mouse N2a neuroblastoma cells were grown at 37°C in a humidified incubator chamber under an atmosphere of 5% CO₂ in Dulbecco's Modified Eagle Medium (DMEM, Gibco) supplemented with 10% foetal bovine serum (FBS, Scientifix), 2 mM GlutaMAX (Thermo Fisher Invitrogen) and 50 U/l penicillin/streptomycin (Thermo Fisher Invitrogen). Cells were passaged 1-2 times per week and plated into 8-well chamber slides (Sarstedt) at a density of 30,000 cells/well (0.5 ml medium/well). The cells were transfected 24 h after plating using Lipofectamine LTX + PLUS reagent (Invitrogen) and imaged 2 days later.

Hippocampal neurons were obtained from embryonic day 17 (E17) C57BL/6 mouse embryos with approval from the University of Queensland Animal Ethics Committee. The cells were then plated in 8-well chamber slides coated with poly-D-lysine at a density of 35,000 cells/well (0.5 ml medium/well). Neurobasal medium (Gibco) was used as the plating medium, supplemented with 5% FBS (Gibco), 2% B27, 2 mM GlutaMAX and 50 U/l penicillin/streptomycin. The medium was changed to serum-free Neurobasal medium 24 h post-seeding, and half the medium was changed twice a week. Neurons were transfected using Lipofectamine 2000 (Invitrogen) after 9-10 days *in vitro* (DIV) and imaged 2 days later.

Transfection

DNA plasmids were delivered using Lipofectamine 2000 for primary neurons or Lipofectamine LTX Reagent for N2a cells. We used Mito-KillerRed (Evrogen, #FP964) and Mito-DsRed constructs (kindly provided by Dr. Xiaobing Yuan) for photostimulation experiments, Matrix-roGFP (Addgene, #49437) and Cyto-roGFP (Addgene, #49435) constructs for mitochondrial and cytosolic redox state assessment respectively, and the Perceval construct (Addgene, #21737) for ATP/ADP ratio assessment. The Mito-paGFP construct was generated by inserting the mitochondrial targeting sequence of human cytochrome c oxidase subunit 8 into the pPA-GFP N1 plasmid (Addgene #11909), using the NheI and BamHI restriction sites.

For N2a cell transfection, cells were washed once with PBS and placed in 500 µl OptiMEM medium (Gibco). Up to 2 µg DNA (for co-transfections) was incubated in 100 µl OptiMEM medium with Plus reagent (v/v) and 2 µl LTX Reagent for 15 min at room temperature, after which 50 µl of transfection solution was added to the cells (1 µg DNA/well)

with incubation at 37°C for 3 h. The cells were then washed twice with PBS and the original conditioned medium was replaced.

For transfection of primary hippocampal neurons, up to 2 µg DNA (for co-transfections) was incubated with Lipofectamine 2000 (v/v) in 100 µl Neurobasal medium for 20 min at room temperature, and then added to cells (1µg DNA/well) and incubated at 37°C for 3 h. The cells were then washed once with PBS and the original conditioned medium was replaced. The medium was changed 24 h later and the cells were imaged 48 h after transfection.

Time-lapse imaging

Imaging parameters

Cells were placed in Hank's Balanced Salt Solution (HBSS, Gibco) buffer shortly before the experiment and imaged using a Zeiss LSM710 confocal microscope running the Zen Black software (2012), with an environmental chamber maintaining the culture temperature at 37°C and the CO₂ level at 5%. Single optical sections were obtained using a 40x 1.4NA oil or 63x 1.4NA oil objective with the following parameters: 1024x1024 pixel resolution, zoom 2.5, scan speed 7, line scan average of 2, scan mode bidirectional. As hippocampal neurons could not be maintained for too long in HBSS buffer, the cells were not imaged for more than 1 h. All acquisition settings were kept constant during imaging.

Mito-KillerRed photostimulation

Mito-KillerRed (mt-KR) is a photosensitizer that generates reactive oxygen species (ROS) within mitochondria upon green light activation (excitation: 561 nm – emission: 601 nm) (Bulina et al., 2006). Before imaging, cells expressing mt-KR were protected from light to prevent inadvertent ROS production. mt-KR photostimulation (photobleaching) was performed by scanning the cells 20 times (0.5 s interval) with a 561 nm laser at 100%. The total length of irradiation did not exceed 30 s. Local photostimulation experiments were performed by activating the mt-KR in the soma or in the dendrites (area = 10 µm²) approximately 50-75 µm from the centre of the soma.

Investigation of mitochondrial and cytosolic redox state

To investigate changes in the mitochondrial and cytosolic reduction/oxidation (redox) environment before and after mt-KR activation, cells were co-transfected with the mt-KR and Matrix-roGFP or cyto-roGFP plasmids coding for redox-sensitive green fluorescent proteins localised to mitochondria or the cytosol, respectively (Waypa et al., 2010). In an oxidised

environment, the excitation increases at short wavelengths (405 nm) at the expense of longer wavelengths (488 nm). The emission wavelength for both states is 525 nm. The ratio of fluorescence intensity at excitation 405 nm/excitation 488 nm therefore indicates oxidation/reduction, with higher ratios reflecting a more oxidized environment. By co-transfecting the cells with the mt-KR and the roGFP plasmids, the redox state was followed in real-time, before and after mt-KR activation in the whole cell or after local mt-KR activation in the soma or dendrite. A 40x oil objective was used to visualize the soma and dendrites of hippocampal neurons. Cells were imaged three times before mt-KR stimulation (baseline), then every 30 s for 5 min after mt-KR stimulation, and finally again twice after 30 min (30 s interval).

Measuring ATP/ADP ratio

To investigate changes in the ATP/ADP ratio before and after mt-KR activation, cells were co-transfected with the mt-KR and Perceval plasmids. Perceval is a genetically encoded green fluorescent biosensor that binds both ATP and ADP, with higher affinity for ATP (Berg et al., 2009). The competition between the two substrates induces a change in the excitation spectrum of the Perceval protein, with a diminished peak at 405 nm and an enhanced peak at 490 nm when the ATP level increases. By co-transfecting the cells with the mt-KR and Perceval plasmids, the ATP/ADP ratio was followed in real-time, before and after mt-KR activation in the whole cell or after local mt-KR activation in the soma or dendrite. A 40x oil objective was used to visualize the soma and dendrites of hippocampal neurons. Cells were imaged every 30 s for 5 min and then again twice after 30 min (30 s interval).

Analysis of mitochondrial dynamics and mobility

To investigate changes in mitochondrial dynamics and mobility before and after mt-KR activation, cells were co-transfected with the mt-KR and mito-photoactivatable GFP (mt-paGFP) plasmids. PaGFP is a photoactivatable protein, the basal absorbance of which is decreased, allowing for the fluorescence to be “switched on” (Karbowski et al., 2004, Patterson and Lippincott-Schwartz, 2002). Photoactivation by UV light (around 400 nm) leads to a 100-fold increase in fluorescence intensity, which can be used to study mitochondrial dynamics as well as changes in the local mitochondrial network.

The mt-KR was imaged using a 63x oil objective before photostimulation / mt-paGFP activation in order to assess the fluorescence baseline. To prevent mt-KR-induced ROS production during imaging, the 561 nm laser power was decreased to 0.5%. A 10 μm^2 region of interest (ROI) was selected for photostimulation with the mt-KR and directly followed by mt-

paGFP photoactivation. The mt-paGFP was imaged every 5 s for 8 min using 488 nm excitation (63x oil objective) in order to assess the mobility of damaged mitochondria in the stimulated region and surrounding zones in the soma and dendrites. The mt-KR and mt-paGFP were imaged immediately after stimulation/activation (T=0 min) and then every 10 min for 30 min to investigate the mitochondrial dynamics. The mito-DsRed (mt-DS) was used as a negative control.

Image analysis

All images were analyzed using Fiji (version 2.0.0), an NIH ImageJ software focused on biological image analysis (Schindelin et al., 2012).

For the analysis of mitochondrial and cytosolic redox state as well as ATP/ADP ratio, ROIs were drawn in different neuronal compartments (see also Fig3A and 3E) as well as in background regions outside the neuron. The pixel intensity was measured for each time point on images taken at two wavelengths, 405 nm and 488 nm, before and after mt-KR stimulation, and background subtracted. The fluorescence ratio 405 nm/488 nm reflects the redox environment (roGFP experiments), with an increase in the ratio indicating oxidation. The fluorescence ratio 488 nm / 405 nm reflects the ATP/ADP ratio (Perceval experiments), with a decrease in the ratio indicating a decrease in the ATP level. For the generation of fluorescence ratio images, the 488 nm channel was manually ‘thresholded’ and ‘binarized’ to serve as a segmentation mask as previously described (Breckwoldt et al., 2014). The same mask was used to segment both channels (405 and 488 nm), which had been previously background-subtracted. The resulting images were then divided using the “Image calculator” on Fiji. The look-up table “16_colors” was used to display images (used only for representation).

The analysis of mitochondrial morphology was performed with an automated image processing and morphometry macro in Fiji as previously described (Merrill et al., 2017). Briefly, images were background-subtracted (rolling ball radius = 50 pixels) and uneven labelling of mitochondria was improved through local contrast enhancement using contrast-limited adaptive histogram equalization (“CLAHE”). To segment mitochondria, the “Tubeness” filter was applied. After setting an automated threshold, the “Analyze Particles” plugin was used to determine the area and perimeter of individual mitochondria and the “Skeletonize” function was used to measure mitochondrial length. The average metrics obtained reflect:

- the mitochondrial elongation or form factor (FF), the inverse of circularity describing a particle’s shape complexity:

$$\text{Form factor} = n^{-1} \sum^n \frac{\text{perimeter}^2}{4\pi\text{area}}$$

- mitochondrial interconnectivity or aspect ratio, the ratio of the major and minor axes of a fitted ellipse:

$$\text{Aspect ratio} = n^{-1} \sum^n \frac{\text{major}}{\text{minor}}$$

- mitochondrial length:

$$\text{Length} = n^{-1} \sum^n \text{area}_{\text{skeleton}}$$

For the analysis of mitochondrial dynamics, three ROIs were selected in the first image collected after mt-paGFP activation (T=0 min, post-activation values): the stimulated ROI (10 μm^2), surrounding area “1” (=zone 1, boundaries approximately 10 μm from the stimulated ROI), and the surrounding area “2” (= zone 2, the rest of the soma or a 20 μm wide area from either side of the surrounding area 1 in the dendrite, see also Figure 5A inset and Figure 6A inset). The mt-paGFP-positive area was measured in zones 1 and 2 to assess the diffusion of the GFP signal, reflecting mitochondrial fusion/content mixing. Specifically, the mt-paGFP-positive area as percentage of total area (zone 1 or zone 2) was measured on the binary images obtained using the same threshold algorithm (“Otsu”, (Otsu, 1979)) on every image. In addition, the fluorescence recovery after mt-KR or mt-DS photostimulation (bleaching) was measured in the stimulated ROI (in the soma or dendrite) as an indicator of mitochondrial movement back into the ROI. The percentage area where the mt-paGFP signal co-localized with the mt-KR or mt-DS signal (red x green) was further assessed as an additional indication of mitochondrial fusion in the stimulated region and surrounding zones. Binary images were obtained using the same threshold algorithm (Otsu) for both channels (red: mt-KR or mt-DS, green: mt-paGFP) and multiplied using the “Image calculator” on Fiji. The resulting binary image reflects the area of red and green co-localization.

To assess the changes in mitochondrial network and dynamics (fusion) occurring 30 min after stimulation, the fluorescence values and percentage area at 30 min were subtracted from those obtained at 0 min (T30 min – T0min).

The mitochondrial mobility within and around the damaged region was assessed using mt-paGFP time-lapse imaging. A straight line of approximately 15 μm was drawn with the photostimulated ROI in the center of the soma or dendrite. Kymographs were generated with the KymographClear plug-in in Fiji which provides automatic color coding of the different

directions of movement (Mangeol et al., 2016). Then, the software KymographDirect was used to perform automated, quantitative analysis of the kymographs obtained with KymographClear as previously described (Mangeol et al., 2016).

Statistical analysis

Graph Pad Prism (version 7.0c) was used for statistical analysis and data presentation. Student's t-test was used to compare two different conditions, a one-way ANOVA with Dunnett's multiple comparisons was used to compare more than two different conditions, and a two-way ANOVA (repeated measurements) with Dunnett's multiple comparison was used to compare the different time points in different neuronal compartments versus the baseline time point (before mt-KR stimulation). Statistical correlations were determined using Pearson's correlation coefficient. A P value of <0.05 was considered statistically significant. Statistical parameters can be found in the figure legends.

Supplemental references

- BERG, J., HUNG, Y. P. & YELLEN, G. (2009). A genetically encoded fluorescent reporter of ATP:ADP ratio. *Nat Methods* 6, 161-6.
- BRECKWOLDT, M. O., PFISTER, F. M., BRADLEY, P. M., MARINKOVIC, P., WILLIAMS, P. R., BRILL, M. S., PLOMER, B., SCHMALZ, A., ST CLAIR, D. K., NAUMANN, R., et al. (2014). Multiparametric optical analysis of mitochondrial redox signals during neuronal physiology and pathology in vivo. *Nat Med* 20, 555-60.
- BULINA, M. E., CHUDAKOV, D. M., BRITANOVA, O. V., YANUSHEVICH, Y. G., STAROVEROV, D. B., CHEPURNYKH, T. V., MERZLYAK, E. M., SHKROB, M. A., LUKYANOV, S. & LUKYANOV, K. A. (2006). A genetically encoded photosensitizer. *Nat Biotechnol* 24, 95-9.
- KARBOWSKI, M., ARNOULT, D., CHEN, H., CHAN, D. C., SMITH, C. L. & YOULE, R. J. (2004). Quantitation of mitochondrial dynamics by photolabeling of individual organelles shows that mitochondrial fusion is blocked during the Bax activation phase of apoptosis. *J Cell Biol* 164, 493-9.
- MANGEOL, P., PREVO, B., PETERMAN, E. J. G. & HOLZBAUR, E. (2016). KymographClear and KymographDirect: two tools for the automated quantitative analysis of molecular and cellular dynamics using kymographs. *Molecular Biology of the Cell* 27, 1948-1957.
- MERRILL, R. A., FLIPPO, K. H. & STRACK, S. (2017). Measuring mitochondrial shape with ImageJ. *Neuroinformatics* 123, 31-48.
- OTSU, N. (1979). A threshold selection method from gray-level histograms. *IEEE Trans. Sys., Man, and Cyber.* 9, 225-236.
- PATTERSON, G. H. & LIPPINCOTT-SCHWARTZ, J. (2002). A photoactivatable GFP for selective photolabeling of proteins and cells. *Science* 297, 1873-7.
- SCHINDELIN, J., ARGANDA-CARRERAS, I., FRISE, E., KAYNIG, V., LONGAIR, M., PIETZSCH, T., PREIBISCH, S., RUEDEN, C., SAALFELD, S., SCHMID, B., et al. (2012). Fiji: an open-source platform for biological-image analysis. *Nat Methods* 9, 676-82.
- WAYPA, G. B., MARKS, J. D., GUZY, R., MUNGAI, P. T., SCHRIEWER, J., DOKIC, D. & SCHUMACKER, P. T. (2010). Hypoxia triggers subcellular compartmental redox signaling in vascular smooth muscle cells. *Circ Res* 106, 526-35.